

The energy dependence of the in-medium ηN cross section evaluated from η -photoproduction *

M. Effenberger and A. Sibirtsev
 Institut für Theoretische Physik, Universität Giessen
 D-35392 Giessen, Germany

Abstract

Within the Glauber formalism and a BUU transport model we analyze the η -photoproduction data from nuclei and evaluate the in-medium ηN cross section. Our results indicate that the ηN cross section is almost independent of the η energy up to 200 MeV.

1 Introduction

For a long time η -meson production in nuclei has been of interest as a source of information about the η -nucleus final state interaction. The present knowledge about the ηN interaction even in the vacuum comes from either simple analysis of the inverse $\pi N \rightarrow \eta N$ reaction or as a free parameter fitted to experimental data by theoretical calculations [1, 2, 3, 4].

Note that the value of the ηN scattering length is still an open problem and there is not actual agreement between a bulk of theoretical investigations.

The analysis of η -production from pA collisions indicated strong sensitivity of the calculations to the prescription of the η -meson final state interaction [3, 5, 6]. It was found that the η -energy spectrum [7] is mostly influenced by the variation of the ηN cross section [5, 6]. However the experimental data [7] had large uncertainties and there was no continuation of the systematical studies.

Recent measurements on η -meson photoproduction in nuclei [8] are more detailed and accurate. Among the theoretical investigations [9, 10, 11] only the calculations within the Distorted Wave Impulse Approximation (DWIA) from Lee et al.[9] are able to reproduce the experimental data by incorporating the η -nucleus potential proposed by Bennhold and Tanabe [12].

The present paper is organized as follows. In section 2 we use the Glauber formalism to extract the in-medium ηN cross section from the experimental data. In section 3 these results are compared to Boltzmann-Uehling-Uhlenbeck transport model calculations. The sensitivity of the theoretical results to the prescription of ηN scattering is investigated.

*Supported by Forschungszentrum Jülich, GSI, BMBF and DFG

2 Analysis within the Glauber Model

In an incoherent approximation the cross section of η -meson photoproduction off nuclei is given by

$$\sigma_{\gamma\eta}^A = \sigma_{\gamma\eta}^p \times [Z + \zeta(A - Z)] \quad (1)$$

with A , Z being the mass and charge of the target, respectively, while the factor $\zeta = 2/3$ [13] stands for the ratio of the elementary η -photoproduction cross sections from γn and γp reactions.

In nuclei the cross section differs from the approximation (1) due to nuclear effects. (i) The Fermi motion of nucleons as well as (ii) Pauli blocking are important at energies below and close to the reaction threshold in free space [14, 15]. We should also take into account (iii) the modification of the N^* -resonance by the nuclear medium [10, 11].

However the most important effect is (iv) the strong final state interaction of η -mesons in nuclear matter. The deviation of the A -dependence of the $\sigma_{\gamma A \rightarrow \eta X}$ from A^1 mostly reflects the strength of the final state interaction.

Here we present an analysis of the experimental data on $\gamma A \rightarrow \eta X$ reactions in order to extract the in-medium cross section $\sigma_{\eta N}$. Our approach is based on the Glauber model [16] and first was developed by Margolis [17] for evaluation of the ρN cross section from both incoherent and coherent ρ -meson photoproduction off nuclei. The most detailed description and application of the Glauber model to photoproduction reactions may be found from review of Bauer, Spital and Yennie [18]. A similar formalism is adopted for studying color transparency [19, 20], where the in-medium cross sections is treated as a function of a transverse separation of the hadronic wave function.

In the Glauber model the cross section of the incoherent η -meson photoproduction reads

$$\sigma_{\gamma\eta}^A = \sigma_{\gamma\eta}^p \frac{Z + \zeta(A - Z)}{A} \times A_{eff} \quad (2)$$

where

$$A_{eff} = \frac{1}{2\pi} \int_0^{+\infty} d\mathbf{b} \int_{-\infty}^{+\infty} dz \rho(\mathbf{b}, z) \int_0^{2\pi} d\phi \exp \left[-\sigma_{\eta N} \oint d\xi \rho(\mathbf{r}_\xi) \right] \quad (3)$$

Here $\rho(r)$ is the single particle density function, which was taken of Fermi type with parameters for each nucleus from [21]. The last integration in Eq. (3) being over the path of the produced η -meson

$$r_\xi^2 = (b + \xi \cos\phi \sin\theta)^2 + (\xi \sin\phi \sin\theta)^2 + (z + \xi \cos\theta)^2 \quad (4)$$

Here θ is the emission angle of the η -meson relative to γ -momentum.

Eq. (3) is similar to those from [22, 23] and in the low energy limit, i.e. by integration over the η -emission angle θ becomes as [24]

$$A_{eff} = \int_0^{+\infty} d\mathbf{b} \int_{-\infty}^{+\infty} dz \rho(\mathbf{b}, z) \exp \left(-\sigma_{\eta N} \int_z^\infty d\xi \rho(\mathbf{b}, \xi) \right) \quad (5)$$

In the high energy limit, i.e. with the small angle scattering approximation $\theta = 0$, Eq. (3) reduces to simple formula from [25]

$$A_{eff} = \frac{1}{\sigma_{\eta N}} \int_0^\infty d\mathbf{b} \left(1 - \exp \left[-\sigma_{\eta N} \int_{-\infty}^{+\infty} dz \rho(\mathbf{b}, z) \right] \right) \quad (6)$$

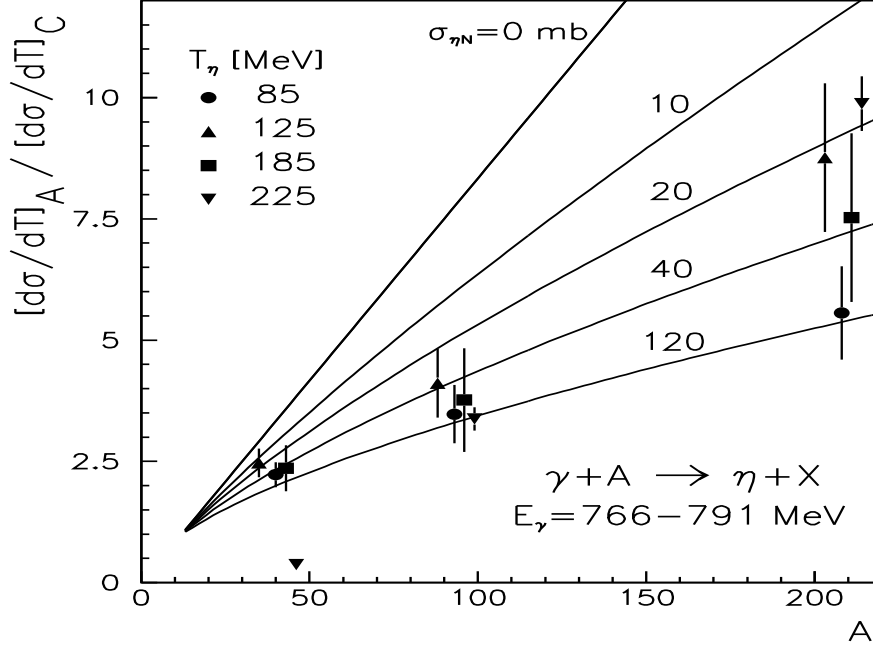


Figure 1: The ratios of the differential cross sections as function of the target mass and for different η -kinetic energies. The experimental data are taken from [8]. Lines show our calculations for several values of $\sigma_{\eta N}$.

The nuclear transparency is defined now as

$$T^A = \frac{\sigma_{\gamma\eta}^A}{\sigma_{\gamma\eta}^p \times [Z + \zeta(A - Z)]} \quad (7)$$

and in the Glauber model it is simply given by

$$T^A = A_{eff}/A \quad (8)$$

being the function of the target mass A , emission angle θ and in-medium ηN cross section $\sigma_{\eta N}$. Note that this model neglect the in-medium effects (*i-iii*), and takes only the final state interactions into account.

We analyze now the recent MAMI data [8] on η -photoproduction from ^{12}C , ^{40}Ca , ^{93}Nb and ^{207}Pb at $E_\gamma < 800$ MeV in order to resolve the dependence (3) with respect to the target mass. The η -production threshold on a free nucleon lies at $\simeq 706$ MeV, thus our analysis is expected to be valid for $E_\gamma \geq 750$ MeV, in order to minimize effects (*i-ii*). Moreover, to minimize the uncertainties related to (*iii*), which also are valid at high E_γ , we analyze the ratios of the differential cross sections integrated over the η -meson emission angle as

$$R(A/^{12}C) = \frac{d\sigma_{\gamma\eta}^A}{dT} \left(\frac{d\sigma_{\gamma\eta}^C}{dT} \right)^{-1} \quad (9)$$

We thus assume that the medium modifications of the N^* -resonance are almost the same for all nuclear targets.

The ratios (9) are shown in Fig. 1 for several kinetic energies of η -mesons and as a function of the target mass. The lines indicate our calculations performed for different ηN cross sections. The model results are integrated over the θ . Note that for $\sigma_{\eta N}=0$ the ratio (9) saturates at $R = A/C$ as was expected neglecting the final state interaction.

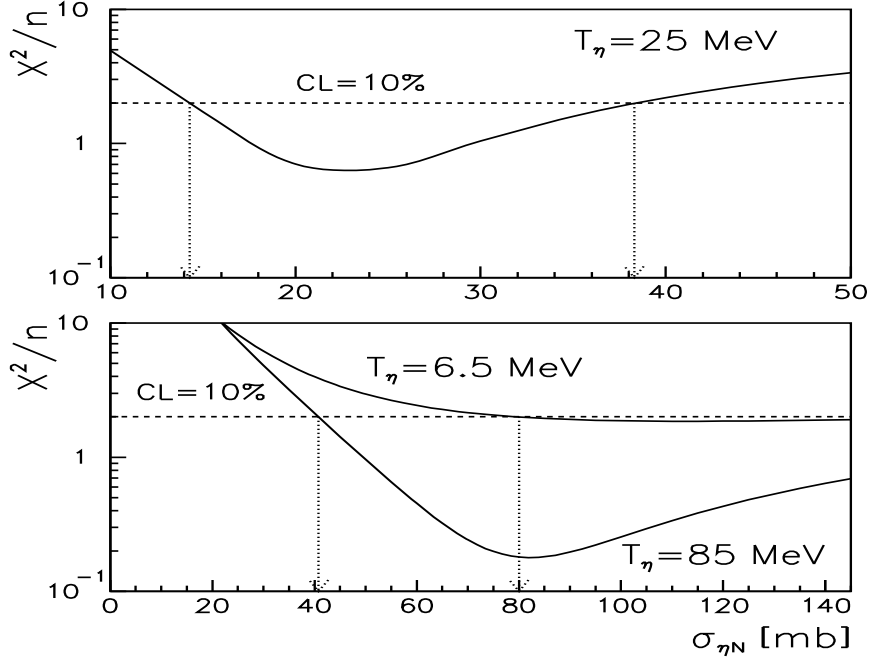


Figure 2: The distribution of reduced χ^2 as function of the ηN cross section.

We now fit the experimental ratios for each T_η by minimizing the χ^2 in order to evaluate $\sigma_{\eta N}$. A similar analysis was performed recently by Kharzeev et al. [26] for the evaluation of the J/Ψ -nucleon cross section. Fig.2 illustrates the minimization procedure and shows sensitivity of the data to the variation of ηN cross section. We fixed the confidence level that gives the value of the reduced $\chi^2/n > 2$ can be expected no more than 10% of the time. With respect to the statistical errors of the experimental data the minimization produces three types of results. Namely, 1) with extraction of $\sigma_{\eta N}$ and indication its uncertainty, 2) with evaluation only the lower limit for $\sigma_{\eta N}$ or 3) with obtaining the minima behind the confidence level.

Fig. 3 shows our final results in comparison with the experimental data and illustrate excellent agreement for wide range of the η -energies. Nevertheless we keep in mind the uncertainties in evaluating of ηN cross section and collect the $\sigma_{\eta N}$ in Fig. 4 as function of the η energy and indication of confidence level. Note that within present analysis we evaluate the inelastic (or absorption) η -nucleon cross section, because the elastic scattering does not remove the η -meson from the total flux, which was detected experimentally.

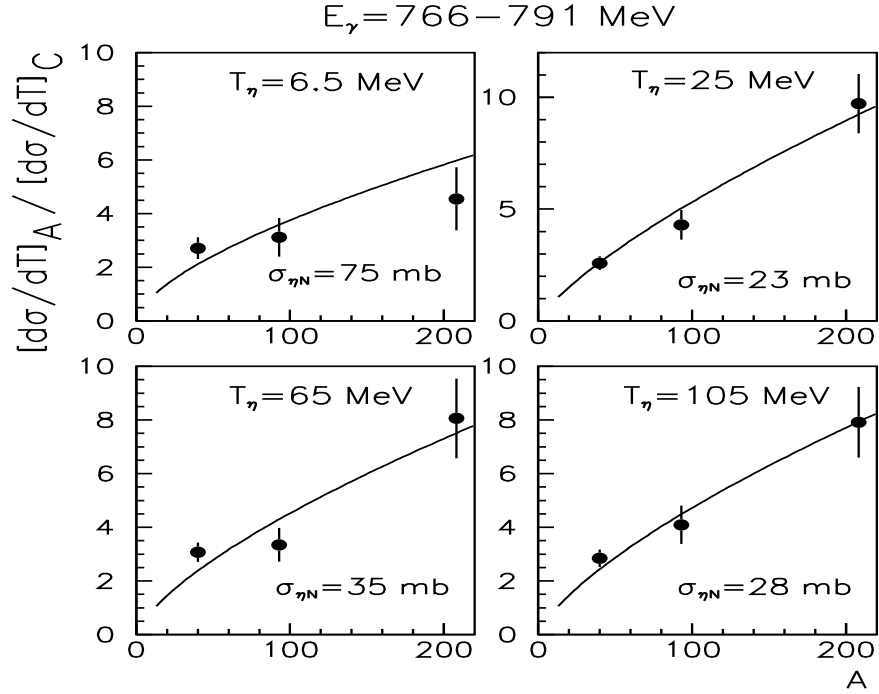


Figure 3: The comparison between experimental data [8] and our fit.

Our results indicate almost constant in-medium ηN cross section as function of the η -energy in strong contradiction with the $\sigma_{\eta N}$ from the scattering in vacuum.

To make a more definite conclusion about the suppression of the ηN cross section in nuclear matter we need an accurate data on the coherent η -photoproduction off nuclei. The coherent reactions are more sensitive to the nuclear transparency ($\propto A_{eff}^2$ [18, 25, 27]) and might solve the uncertainties of the present analysis performed with the Glauber model.

3 Results from BUU calculations

In order to verify the results from the previous section we use a BUU transport model [14, 28, 29] to calculate energy differential η -photoproduction cross sections in nuclei. This allows to drop several assumptions needed for the Glauber calculations. Fermi motion and Pauli blocking are taken into account as well for the primary η -production process as for the final state interaction of the produced particles.

In Ref. [11] the BUU model was used to calculate η -photoproduction in nuclei with the resonance model for the η final state interaction from Ref. [29]. Here the η -rescattering was described by intermediate excitations of $N(1535)$ resonances. The elastic and inelastic ηN cross sections calculated with this model are shown in Fig. 5 with the solid lines. It turned out that this model was able to describe the total η -photoproduction cross sections reasonably well but failed in the description of angular and energy differential cross sections. Compared to the experimental data the

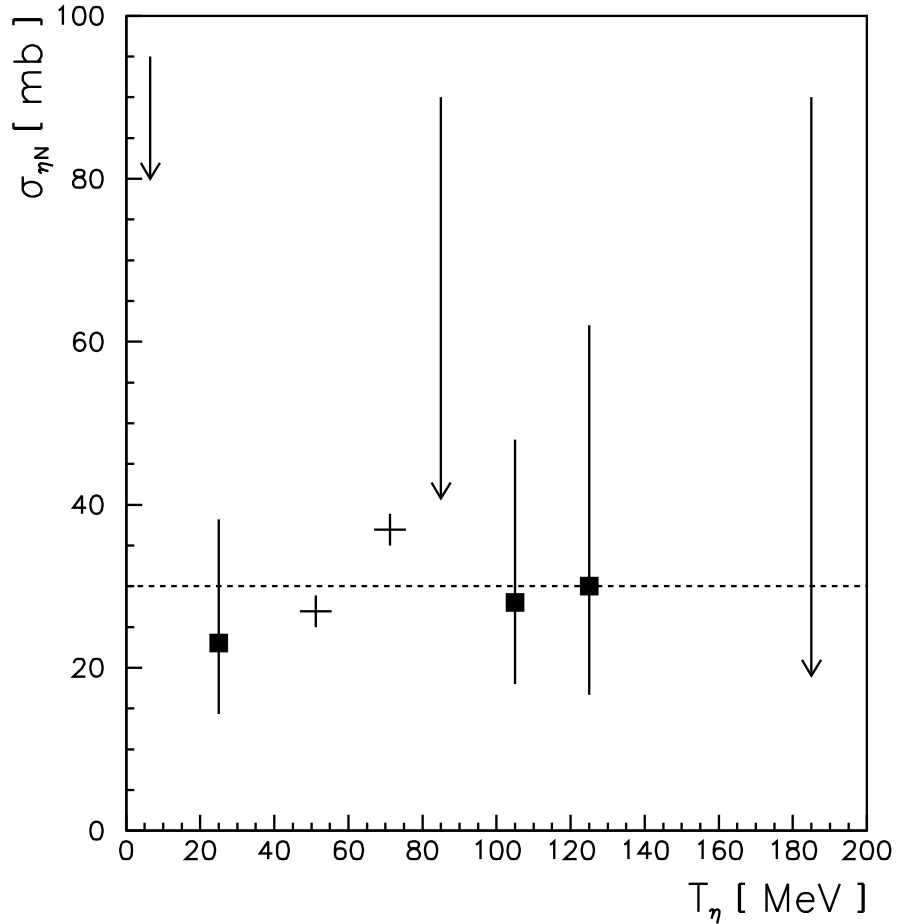


Figure 4: Energy dependence of ηN cross section. Squares indicate the results for the cases when we were able to extract $\sigma_{\eta N}$ within 10% confidence level, arrows when we could only obtain a lower limit for $\sigma_{\eta N}$ and crosses if the result of our analysis is behind the confidence level. The dashed line indicates a constant cross section of 30 mb.

calculated cross sections were shifted to smaller angles and larger η -energies for all considered target nuclei and all photon energies up to 800 MeV. In Fig. 6 the solid line shows the calculation of an energy differential η -photoproduction cross section on ^{40}Ca with this model.

It was already reported in Ref. [11] that the discrepancy to the experimental data is cured by using an energy independent ηN cross section. The corresponding result is shown in Fig. 6 by the line labelled 'constant cross sections (1)' where an inelastic cross section $\sigma_{in}^\eta = 30$ mb and an elastic cross section $\sigma_{el}^\eta = 20$ mb was used.

Now we want to study the influence of different prescriptions for ηN scattering. The dashed line in Fig. 6 indicates the results calculated with a modified η -rescattering

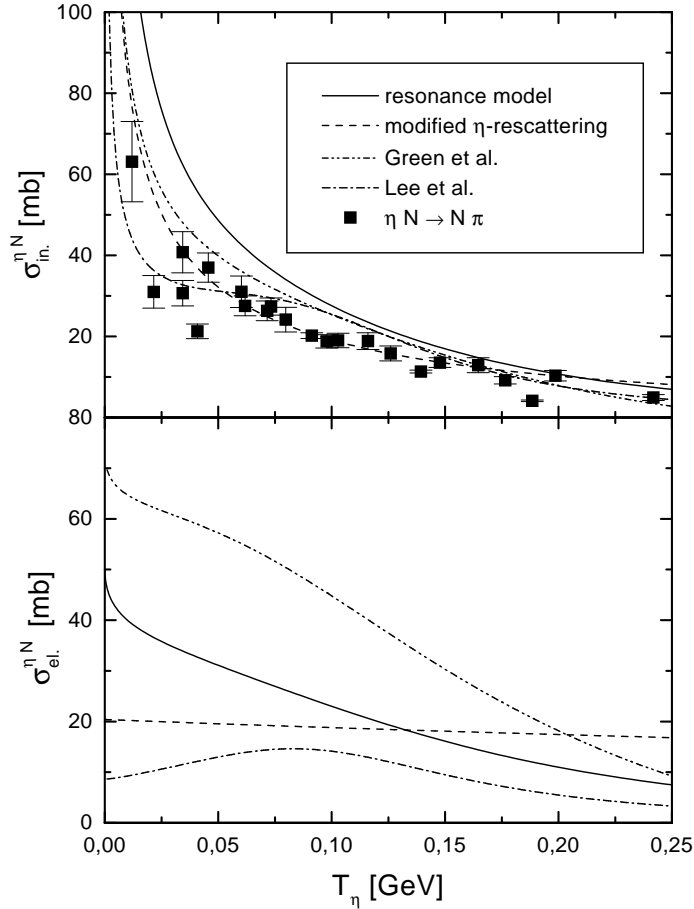


Figure 5: Inelastic and elastic cross sections for ηN scattering with different models. Experimental data points are obtained by detailed balance from $\pi^- p \rightarrow \eta n$ [31]. Note that the theoretical curves for the inelastic cross section can not directly be compared to the data because they contain additional channels.

model:

$$\sigma_{\eta N \rightarrow \pi N} = \frac{q_\pi}{q_\eta s} \frac{c^2}{c^2 + q_\eta^2} 40 \text{ mb GeV}^2, \quad c = 0.3 \text{ GeV} \quad (10)$$

$$\sigma_{\eta N \rightarrow \eta N} = \frac{45 \text{ mb GeV}^2}{s}$$

where q_π , q_η are the cms momenta of the π - and η -meson, respectively, and s stands for the squared invariant energy. The inelastic cross section was obtained by fitting the experimental data for the reaction $\pi N \rightarrow \eta N$, while the elastic cross section was assumed to be equal to the one in the resonance model at an η -energy of 125 MeV. The resulting elastic and inelastic cross sections are shown in Fig. 5 with the dashed

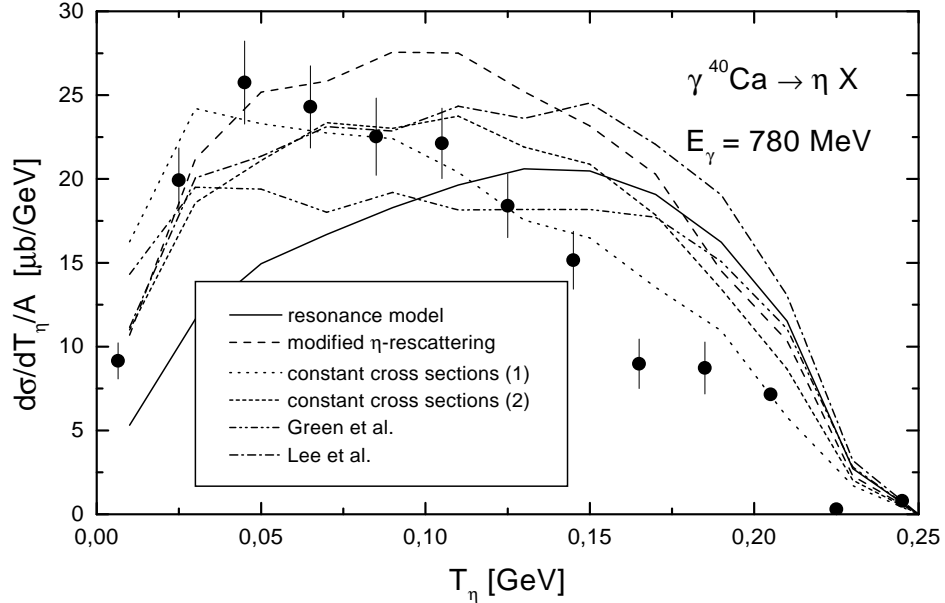


Figure 6: Energy differential η -photoproduction cross sections for $E_\gamma = 780$ MeV in ^{40}Ca . Experimental data are from [8]. Lines indicate BUU calculations with ηN cross sections as described in the figure. For further explanations see text.

line. As can be seen from Fig. 6 (dashed line) this model improves the description of the energy differential cross section for small η -energies but still overestimates the cross section for higher energies.

We have also used the ηN cross sections from Green and Wycech [30] and Lee et al. [9]. The calculation of Green and Wycech is based on the K-matrix method and includes the $S_{11}(1535)$ and $S_{11}(1650)$ resonances. Following the authors this model is valid up to an invariant energy of about 100 MeV from ηN threshold which corresponds to an η kinetic energy in the nucleon rest frame of 160 MeV. Lee et al. use a parameterization of the ηN scattering amplitude that is based on the calculation of Bennhold and Tanabe [12]. This model contains the $P_{11}(1440)$, $D_{13}(1520)$ and $S_{11}(1535)$ resonances and might therefore be limited to an η kinetic energy of about 100 MeV.

The total cross sections within these models are shown in Fig. 5. Both models give about the same inelastic cross section which is basically due to the fact that in both models the dominating inelastic channel is given by the process $\eta N \rightarrow N\pi$. The experimental data [31] for this reaction, obtained by detailed balance from $\pi^- p \rightarrow \eta n$, are also shown. But one should note that the theoretical curves contain additional, even though small, contributions from $\eta N \rightarrow N\pi\pi$ and therefore can not directly be compared to these data points. The elastic ηN cross section in both models is very different which is an indication for the large theoretical uncertainties in the models for ηN scattering even in the vacuum.

The corresponding results of the BUU calculations for photoproduction are given in Fig. 6. As in the calculations within the resonance model and the model from Eq. (10) we again fail to describe the shape of the energy differential cross section. The same holds for all target nuclei and photon energies as well as for the angular differential cross sections. Apart from the resonance model [29] all models give a satisfactory description of the cross section for η -energies below 50 MeV. The failure of the resonance model is due to the fact that this model was fitted to a larger class of elementary processes and a wider kinematical range and overestimated the cross section for $\eta N \rightarrow N\pi$ in the considered energy range.

In Fig. 6 we also show the result of a model calculation with a constant inelastic cross section $\sigma_{in}^{\eta} = 30$ mb where we neglected elastic ηN scattering (curve labelled 'constant cross sections (2)'). Compared to the previous calculation with constant cross sections that included an elastic cross section the energy differential cross section is shifted to larger energies and fails to describe the data. Moreover the integrated cross section is slightly larger because the elastic cross section increases, in average, the length of the path of the produced etas through the nucleus and therefore reduces the number of etas that escape from the nucleus. One sees that in our model a constant inelastic ηN cross section alone is not sufficient to describe the data but an elastic cross section is also needed.

Since the models for ηN scattering in the vacuum show a rather strong decrease of the total ηN cross section with η -energy we are not able to reproduce the data for η -photoproduction with any of these models within our transport model approach. For η -energies larger than 100 MeV we need an ηN cross section that is significantly larger than the one from the vacuum models while for lower energies our calculations are not very sensitive to the size of the cross section. A possible explanation is that the vacuum models [30, 12] are simply not applicable to the considered energy range. After all, due to the Fermi motion of the nucleons, the ηN cross section up to an invariant energy of $\sqrt{s} = 1.74$ GeV ($T_{\eta} = 446$ MeV in the nucleon rest frame) enters the calculations for an eta with a kinetic energy of 250 MeV in the rest frame of the nucleus.

Our findings are in line with the Glauber analysis from section 2 and Ref. [8] which need a constant inelastic cross section of 30 mb in order to describe the mass dependence of the energy differential cross sections. However, Lee et al. [9] were able to reproduce energy differential cross sections within the DWIA framework by using vacuum ηN cross sections. One crucial difference to our calculation is that in their calculation the outgoing nucleon in the elementary photoproduction process $\gamma N \rightarrow N\eta$ is set on-shell while in our semi-classical treatment the elementary process takes place instantaneously with following propagation of the produced particles through the nucleus. The potential energy which is needed to set the nucleon on-shell clearly shifts the η -spectrum to lower energies. A priori it is not obvious which of the two prescriptions is better suited to model the physical reality. Only a DWIA calculation along the line of Ref. [32] without the local approximation of Ref. [9] could clarify this question. An indication for a larger ηN cross section at higher energies is the fact that we are able to describe energy and angular differential cross section for η -photoproduction simultaneously by using a constant cross section [11] while in the calculations of Lee et al. the angular differential cross sections are shifted to smaller angles compared to the data.

4 Summary

We have analyzed the η -photoproduction in nuclei within the framework of the Glauber model and a BUU transport model approach.

Using the standard Glauber theory we investigate the A -dependence of the reaction $\gamma A \rightarrow \eta X$ in order to extract the data on η -meson final state interaction in nuclei. It was found that the in-medium ηN cross section is almost energy independent from $\eta N \rightarrow \pi N$ threshold up to η -kinetic energy of 130 MeV.

Within a BUU transport model calculation we are able to reproduce energy and angular differential data for η photoproduction only by using an energy independent ηN cross section but not with any available ηN vacuum cross section. However, the effect of the nucleon potential that can not be treated in our semi-classical calculation in a correct way might have an impact on that conclusion.

5 Acknowledgement

The authors are grateful to B. Krusche and H. Stroeher for productive discussions. They especially like to thank U. Mosel for valuable suggestions and a careful reading of the manuscript.

References

- [1] R.S. Bhalerao and L.C. Liu, Phys. Rev. Lett. 54 (1985) 865.
- [2] C. Wilkin, Phys. Rev. C 47 (1993) R938.
- [3] E. Chiavassa et al. Z. Phys. A 344 (1993) 345.
- [4] A.A. Sibirtsev, Phys. Scr. RS 21 (1993) 167.
- [5] Ye.S. Golubeva, A.S. Ilijnov, E.Y. Paryev and I.A. Pshenichnov, Z. Phys. A 345 (1993) 223.
- [6] A.A. Sibirtsev, Phys. At. Nucl. 56 (1993) 608.
- [7] E. Chiavassa et al., Nuovo Cim. A 107 (1994) 1195.
- [8] M. Roebig-Landau, J. Ahrens, G. Anton et al., Phys. Lett. B 373 (1996) 45.
- [9] F.X. Lee, L.E. Wright, C. Bennhold and L. Tiator, Nucl. Phys. A 603 (1996) 345.
- [10] R.C. Carrasco, Phys. Rev. C 48 (1993) 2333.
- [11] M. Effenberger, A. Hombach, S. Teis and U. Mosel, Nucl. Phys. A 614 (1997) 501.
- [12] C. Bennhold and H. Tanabe, Nucl. Phys. A 530 (1991) 625.
- [13] B. Krusche et al., Phys. Lett. B 358 (1995) 40.

- [14] W. Cassing, V. Metag, U. Mosel and K. Niita, *Phys. Rep.* 188 (1990) 363.
- [15] L.L. Salcedo, E. Oset, M.J. Vicente-Vacas and C. Garcia-Recio, *Nucl. Phys. A* 484 (1988) 557.
- [16] R.J. Glauber and J. Mathiaie, *Nucl. Phys. B* 21 (1970) 135.
- [17] B. Margolis, *Phys. Lett. B* 26 (1968) 254.
- [18] T.H. Bauer, R.D. Spital and D.R. Yennie, *Rev. Mod. Phys.* 50 (1978) 261.
- [19] J. Bertch, S.J. Brodsky, A.S. Golhaber and J.G. Gunion, *Phys. Rev. Lett.* 47 (1981) 297.
- [20] B.Z. Kopeliovich and B.G. Zakharov, *Phys. Lett.* 264 (1991) 434.
- [21] C.W. Jager, C. Vries and H. Vries, *At. Data Nucl. Data Tables* 14 (1974) 480.
- [22] E. Vercellin, E. Chiavassa, G. Dellacasa et al., *Nuovo Cim. A* 106 (1993) 861.
- [23] J. Hüfner, B. Kopeliovich and J. Nemchik, *nucl-th/9605007* (1996)
- [24] O. Benhar, B.Z. Kopeliovich, C. Mariotti, N.N. Nikolaev and B.G. Zaharov, *Phys. Rev. Lett.* 69 (1992) 1156.
- [25] K.S. Kölbig and B. Margolis, *Nucl. Phys. B* 6 (1968) 85.
- [26] D. Kharzeev, C. Lourenco, M. Nardi and H. Satz, *Z. Phys. C* 74 (1997) 307.
- [27] G. Bochman, B. Margolis and C.L. Tang, *Phys. Lett. B* 30 (1969) 254.
- [28] G.F. Bertsch, H. Kruse and S. Das Gupta, *Phys. Rev. C* 29 (1984) 673.
- [29] S. Teis, W. Cassing, M. Effenberger, A. Hombach, U. Mosel and Gy. Wolf, *Z. Phys. A* 356 (1997) 421.
- [30] A.M. Green and S. Wycech, *Phys. Rev. C* 55 (1977) 2167.
- [31] Baldini et al., *Landolt-Börnstein, Band 12* (Springer, Berlin, 1987).
- [32] X. Li et al., *Phys. Rev. C* 48 (1993) 816.